Journal of Animal Science, 2024, **102**, skae339
https://doi.org/10.1093/jas/skae339
Advance access publication 5 November 2024
Metabolism and Metabolomics

Cecal metabolomics of 2 divergently selected rabbit lines revealed microbial mechanisms correlated to intramuscular fat deposition

Agostina Zubiri-Gaitán[1,*], Marina Martínez-Álvaro[1], Agustín Blasco[1], and Pilar Hernández[1,*]

[1]Institute for Animal Science and Technology, Universitat Politècnica de València, Camino de Vera s/n, Valencia, Spain
*Corresponding authors: agzugai1@upvnet.upv.es (Agostina Zubiri-Gaitán); phernan@dca.upv.es (Pilar Hernández)

Abstract

The gastrointestinal microbiota plays a key role in the host physiology and health through a complex host–microbiota co-metabolism. Metabolites produced by microbial metabolism can travel through the bloodstream to reach distal organs and affect their function, ultimately influencing the development of relevant production traits such as meat quality. Meat quality is a complex trait made up of a number of characteristics and intramuscular fat content (**IMF**) is considered to be one of the most important parameters. In this study, 52 rabbits from 2 lines divergently selected for IMF (high-IMF (H) and low-IMF (L) lines) were used to perform an untargeted metabolomic analysis of their cecal content, with the aim to obtain information on genetically determined microbial metabolism related to IMF. A large, correlated response to selection was found in their cecal metabolome composition. Partial least squares discriminant analysis was used to identify the pathways differentiating the lines, which showed a classification accuracy of 99%. On the other hand, 2 linear partial least squares analyses were performed, one for each line, to extract evidence on the specific pathways associated with IMF deposition within each line, which showed predictive abilities (estimated using the Q^2) of approximately 60%. The most relevant pathways differentiating the lines were those related to amino acids (aromatic, branched-chain, and gamma-glutamyl), secondary bile acids, and purines. The higher content of secondary bile acids in the L-line was related to greater lipid absorption, while the differences found in purines suggested different fermentation activities, which could be related to greater nitrogen utilization and energy efficiency in the L-line. The linear analyses showed that lipid metabolism had a greater relative importance for IMF deposition in the L-line, whereas a more complex microbial metabolism was associated with the H-line. The lysophospholipids and gamma-glutamyl amino acids were associated with IMF in both lines; the nucleotide and secondary bile acid metabolisms were mostly associated in the H-line; and the long-chain and branched-chain fatty acids were mostly associated in the L-line. A metabolic signature consisting of 2 secondary bile acids and 2 protein metabolites was found with 88% classification accuracy, pointing to the interaction between lipid absorption and protein metabolism as a relevant driver of the microbiome activity influencing IMF.

Lay Summary

Genetic determination of phenotypes depends not only on the host genome but also on its microbiome, particularly that of the intestinal tract. Host and microbiome form a complex co-metabolism that ultimately affects relevant phenotypes, like the intramuscular fat content. The metabolomic analysis of the gut content can provide a functional characterization, giving a better insight into the microbiome activity implicated. The objective of this study was to unveil the genetically determined microbial metabolic pathways related to intramuscular fat deposition, a key meat quality trait in all species. To do so, the cecal metabolomic analysis of 2 rabbit lines divergently selected for intramuscular fat content was performed. Important differences between the divergent lines were found in their cecum metabolome, which pointed to the metabolism of secondary bile acids, purines, and several amino acids as the most relevant microbial pathways differentiating the intramuscular fat deposition of the lines. Additional analyses also suggested that there were different microbial pathways associated with the intramuscular fat deposition within each line. Finally, a biomarker composed of 4 microbial metabolites and with 88% classification accuracy was proposed, which pointed to lipid absorption and protein metabolism as relevant drivers of the microbiome activity influencing intramuscular fat deposition.

Key words: intramuscular fat, microbial activity, metabolomics, microbiome, rabbits

Abbreviations: AAA, aromatic amino acids; *alr*, additive log-ratio; β, regression coefficient; BCAA, branched-chain amino acids; BCFA, branched-chain fatty acids; CMV, cross-model validation; CV, cross-validation; $D_{H\text{-}L}$, difference between lines; ESI, electrospray ionization; GGT, γ glutamyltransferase; GWAS, genome-wide association study; H, high-IMF; HESI, heated electrospray ionization source; HILIC, hydrophilic interaction liquid chromatography; $HPD_{95\%}$, highest posterior density interval at 95%; *ilr*, isometric log-ratio; IMF, intramuscular fat; L, low-IMF; LC, long-chain; LTL, Longissimus Thoracis et Lumborum; NIRS, near-infrared spectroscopy; P_0, probability of the difference of being greater or lower than zero; PLS, partial least square; PLS-DA, partial least square-discriminant analysis; RP, reverse phase; SFA, saturated fatty acids; PB, purine bases; PD, purine derivatives; UPLC-MS/MS, ultra-performance liquid chromatography coupled with tandem mass spectrometry; VIP, variable importance in projection

Received April 18, 2024 Accepted November 4, 2024.

Introduction

The gastrointestinal microbiota plays a key role in the host's physiology and health through a complex host–microbiota co-metabolism. The biochemical pathways of the microbiota produce multiple compounds (i.e., metabolites) that can travel through the bloodstream to reach distal organs and influence their function, similar to an endocrine organ (Clarke et al., 2014), ultimately influencing the development of relevant production traits such as meat quality.

Meat quality is a complex trait, as it is made up of several characteristics (Warner et al., 2010; Warris, 2010). The intramuscular fat content (**IMF**) is considered one of its main parameters because it affects the tenderness, juiciness, and flavor of meat, among other characteristics (Warris, 2010), ultimately affecting consumers' acceptability (Frank et al., 2016). It is now known that gut microbiota contributes to fat deposition in humans (Bäckhed et al., 2004; Turnbaugh et al., 2006) and other animal species (Maltecca et al., 2019; Krause et al., 2020; Jing et al., 2022), for example by increasing energy harvest from the diet (Turnbaugh et al., 2006), altering the appetite by modulating satiety hormones (Larraufie et al., 2018; Lim et al., 2020), or acting as a mediator of inflammatory status (Cani et al., 2008; Cussotto et al., 2020; Lim et al., 2020). Consequently, the role of the microbiome in the deposition of IMF, a key parameter in meat quality, has also been explored in multiple species like pigs (Fang et al., 2017), cattle (Krause et al., 2020), sheep (Xie et al., 2022), chicken (Jing et al., 2022) and rabbits (Martínez-Álvaro et al., 2021). The biological mechanisms that the microbiota employs to affect fat deposition are still under elucidation, although some key players have been suggested like short-chain fatty acids (Larraufie et al., 2018), bile acids (Wahlström et al., 2016), branched-chain amino acids (**BCAA**) (Ridaura et al., 2013), among others. Metagenomics (i.e., the high-throughput sequencing of the microbiome) and 16S (i.e., the sequencing of the variable regions of the 16S rRNA gene) analyses have been the cornerstone for these studies; however, the abundance of genes or taxa is not sufficient to understand the microbial metabolism and its crosstalk with the host, one of the reasons being because they do not differentiate between total and active microbes (Fricker et al., 2019). In that scenario, metabolomics analyses have gained special attention due to the fact that metabolites constitute the last response of biological systems to genetic and environmental effects (Fiehn, 2002); therefore, their analysis can be useful to elucidate the metabolic pathways directly related to the phenotype of interest. The metabolomic analysis of the gut content would provide a functional characterization of the microbiome (Marcobal et al., 2013; Zierer et al., 2018), giving a better insight into its biological mechanisms that ultimately affect IMF deposition.

The gut microbiota composition is partially modulated by the host's genes (Bonder et al., 2016; Lim et al., 2020; Lopera-Maya et al., 2022), but it is also highly affected by environmental factors (Rothschild et al., 2018), and the dissociation of such effects is complicated. In this study, animals from 2 rabbit lines divergently selected for IMF in the Longissimus thoracis et lumborum (***LTL***) muscle were used to perform a metabolomic analysis of their cecal microbiota. The divergent selection started from the same base population and the lines were contemporarily reared under the same environmental conditions (including the same diet), making them valuable animal material to study the genetic effect of the trait under selection and the correlated ones, independently from the environment. In rabbits, the analysis of the cecal metabolome is of particular interest due to their cecotrophic behavior, which is essential for their nutritional wellbeing. As hindgut fermenters, their fermentation compartment is located after the enzymatic digestion area. Hence, the ingestion of cecotrophes allows them to recycle a large proportion of the nutrients produced during cecal fermentation, which can represent up to 18% of their dry matter intake and 30% of their daily nitrogen intake (Hörnicke, 1981). Previous studies on the microbiome composition (Martínez-Álvaro et al., 2024) and its metagenome (Martínez-Álvaro et al., 2021) have been carried out on these lines, indicating an important role of the microbiome in fat deposition, which can be directly related to their genetic composition. Additionally, the analysis of their plasma metabolome revealed several metabolic routes that are known to be related to microbiome metabolism (Zubiri-Gaitán et al., 2023). Therefore, in this study, the divergent lines were used to perform an untargeted metabolomics analysis of their cecal content, with the aim of providing a genetically determined functional characterization of the microbiome related to IMF deposition.

Material and Methods

Animals

The Research Ethical Committee of the Universitat Politècnica de València approved all experimental procedures according to Council Directives 98/58/EC and 2010/63/EU (reference number 2017/VSC/PEA/00212).

Rabbits from 2 lines divergently selected for IMF content in the *LTL* muscle were used in this experiment. The selection criterion was the average IMF content of two 9 wk-old rabbits of the first parity of each doe (1 male and 1 female). The selection started from the same base population, and the animals were selected for higher (H: high-IMF line) and lower (L: low-IMF line) IMF content, following the procedure described in previous studies (Zomeño et al., 2013; Martínez-Álvaro et al., 2016). Animals were housed at the experimental farm of the Universitat Politècnica de València. The lines were contemporarily reared, shared the same environmental conditions, and were fed the same diet, ensuring that the differences found between them are mainly due to genetic causes.

Rabbit meat is characterized by a low-fat content, *LTL* being the leanest muscle, with an average of 1 g IMF/100 g of fresh meat (Pla et al., 2010). This divergent selection experiment was successful, showing a response to selection in the 10th generation of 0.49 g IMF/100 g of *LTL*, equivalent to 3.8 SD of the trait. The high-IMF line had a mean of 1.31 g IMF/100 g of *LTL* ($HPD_{95\%}$: [1.27 to 1.34]), while that of the low-IMF line was 0.82 g IMF/100 g of *LTL* ($HPD_{95\%}$: [0.78 to 0.86]), after adjustment for systematic effects as described in Zubiri-Gaitán, et al. (2022a). Correlated responses to selection were also found in IMF content of other muscles with different oxidative patterns (Martínez-Álvaro et al., 2018a), and in total carcass fat content (Zubiri-Gaitán et al., 2022a). However, no differences were found between lines on carcass weight (Zubiri-Gaitán et al., 2022a).

For this study, the cecal metabolome was quantified in 27 rabbits from the H-line (13 males and 14 females) and 25 from the L-line (13 males and 12 females) randomly selected

from the 10th generation of selection (Supplementary Table 1). No cross-fostering was practiced at birth. The litters were weaned at 28 d and then housed jointly within litters. The housing ventilation was controlled, and the photoperiod was constant (16:8 h). The animals were fed ad libitum until slaughter with a standard pelleted commercial diet (NANTA, Madrid, Spain) containing 16.5% crude fiber, 16% crude protein, 7.6% ashes, 2.4% fat, and 0.8% calcium; and supplemented with vitamin A (10,000 UI/kg), vitamin D3 (900 UI/kg), vitamin E (25 mg/kg), iron (78 mg/kg), cobalt carbonate (0.30 mg/kg), manganese (20 mg/kg), zinc (50 mg/kg), selenium (0.05 mg/kg), potassium iodide (1.0 mg/kg), copper (8 mg/kg), and bacitracin zinc antibiotic (100 ppm). The fatty acid composition of the diet, expressed as a percentage of total fatty acids, was 16.6% C16:0, 0.5% C16:1, 1.8% C18:0, 19.7% C18:1, 54.8% C18:2, 5.7% C18:3 and 0.9% fatty acids with more than 20 carbon atoms (C > 20).

Cecum metabolome

The animals were slaughtered at 9 wk of age after 4 h of fasting by electrical stunning and exsanguination. The intestinal tract was immediately removed, cecal content was collected in a sterile 50 mL Falcon tube and stirred until homogenization. Subsequently, it was aliquoted in 2 mL cryogenic tubes and frozen immediately by submersion in liquid nitrogen. The samples were then stored at −80 °C until they were sent to Metabolon, Inc. laboratory (Morrisville, North Carolina, USA) for their analysis. The metabolomic profile was obtained using ultra-performance liquid chromatography (ACQUITY UPLC System, Waters Corp., Milford, USA) coupled with tandem mass spectrometry (Q-Exactive Orbitrap, Thermo Fisher Scientific, Waltham, MA, USA) (UPLC-MS/MS), interfaced with a heated electrospray ionization source (HESI-II). The Orbitrap mass analyser operated at 35,000 mass resolution. This analysis was performed under different conditions to capture metabolites with a wide range of classes and polarities. Sample preparation and analysis steps are thoroughly described below.

The samples were prepared using the automated MicroLab STAR® system (Hamilton Company, Reno, Nevada, USA). The proteins were precipitated with methanol under vigorous shaking for 2 min (Glen Mills GenoGrinder 2000) followed by centrifugation. The resulting extract was divided into 4 aliquots for different analyses: 2 reverse phase (**RP**)/UPLC-MS/MS with positive ion mode electrospray ionization (ESI), one RP/UPLC-MS/MS with negative ion mode ESI, and one hydrophilic interaction liquid chromatography (HILIC)/UPLC-MS/MS with negative ion mode ESI. Samples were placed on a TurboVap® (Zymark, Hopkinton, MA, USA) to remove the organic solvent and finally stored overnight under nitrogen before analysis. The sample extracts were then reconstituted in solvents compatible with the 4 methodologies, which also contained a series of standards to ensure injection and chromatographic consistency.

The first aliquot was gradient eluted from a C18 column (Waters UPLC BEH C18-2.1 × 100 mm, 1.7 µm) using water and methanol, containing 0.05% perfluoropentanoic acid (PFPA) and 0.1% formic acid (**FA**), and analyzed under acidic positive conditions chromatographically optimized for more hydrophilic compounds (identified as *positive-early*). The second aliquot was gradient eluted from the same C18 column using methanol, acetonitrile, water, 0.05% PFPA and 0.01% FA, and analyzed using acidic positive conditions, but chromatographically optimized for more hydrophobic compounds (identified as *positive-late*). The third aliquot was gradient eluted from a separate C18 column using methanol and water, with 6.5 mM ammonium bicarbonate at pH 8, and analyzed using basic negative conditions (identified as *negative*). The last aliquot was eluted from a HILIC column (Waters UPLC BEH Amide 2.1 × 150 mm, 1.7 µm) using a gradient consisting of water and acetonitrile with 10 mM ammonium formate at pH 10.8 and it was analyzed by negative ionization (identified as *polar*). The MS/MS analysis was performed alternating MS and data-dependent MS^n scans using dynamic exclusion. The scan range varied between methods but covered 70-1000 m/z.

Several quality controls (**QC**) were analyzed together with the experimental samples: a pooled matrix composed by a small volume of each experimental sample served as a technical replicate; extracted water samples served as process blanks; and a pool of QC standards were spiked into every analyzed sample, to monitor instrument performance and aid in the chromatographic alignment.

Raw data were extracted from the 4 analyses (*positive-early*, *positive-late*, *negative*, and *polar*). Metabolon, Inc. laboratory was responsible for the detection of peaks, the processing of the QC, and the identification of the compounds by comparison to library entries of purified standards or recurrent unknown entities. The identification was based on 3 criteria: retention index, accurate mass match to the library (+/- 10 ppm), and the MS/MS forward and reverse scores between the experimental data and authentic standards. Peaks were quantified using area-under-the-curve. Finally, the information regarding the function and metabolic pathways of each metabolite identified came from the Human Metabolome Database and the Kyoto Encyclopedia of Genes and Genomes database.

Data processing

The dataset of each methodology was processed separately as follows: after some exploratory analyses, the metabolites that were undetected (i.e., intensity = 0) in more than 20% of the samples were removed, and the remaining zeros were imputed using random forest with the R package missForest (Stekhoven and Bühlmann, 2011). An additive log-ratio transformation (*alr*) was then applied using the R package easyCODA (Greenacre, 2018). The *alr* is applied to account for the fact that metabolomics data are compositional since they carry relative, rather than absolute, information (Kapoore and Vaidyanathan, 2016; Alseekh et al., 2021). The *alr* is defined as:

$$\ln\left(\frac{x_j}{x_{\text{ref}}}\right) = \ln\left(x_j\right) - \ln\left(x_{\text{ref}}\right), \quad j = 1, \ \ldots, J-1, \ j \neq \text{ref}$$

where x_j is the abundance of the jth metabolite, x_{ref} is the abundance of a reference metabolite and J is the total number of metabolites in the dataset. The reference metabolite was chosen following the methodology proposed by Greenacre et al. (2021), which consists of choosing the metabolite that 1) reproduces the geometry of the full set of log-ratios in a Procrustes analysis (measured with the Procrustes correlation), and 2) has low variance, ensuring that the main variation is due to the numerator. The metabolites chosen for the 4 datasets mentioned above had a Procrustes correlation >0.99 and were: methionine for the *positive-early* dataset, stearoyl

ethanolamine for the *positive-late* dataset, N-acetyl leucine for the *negative* dataset, and 2R,3R-dihydroxybutyrate for the *polar* dataset. Once transformed, the 4 datasets were joined to proceed with the statistical analysis.

Statistical analysis and validation

Two multivariate approaches were used to identify the differences between lines in the microbiome activity: a partial least square-discriminant analysis (**PLS-DA**), for which the *y* vector was categorical, coding the H or L-line, and a linear PLS analysis, for which the *y* vector contained the IMF content. Previous studies performed on these lines have suggested that the metabolic routes that led to greater IMF content in the H-line, and lower IMF content in the L-line may not be identical (Zubiri-Gaitán et al., 2023) which means that the metabolites that adjust linearly to the IMF in each line can partially differ. Therefore, in this study, 2 different PLS were performed, one with the samples from the H-line (PLS-H) and the other with the samples from the L-line (PLS-L). All analyses were performed after scaling the dataset to mean 0 and SD 1, using the R package mdatools (Kucheryavskiy, 2020).

A cross-model validation (**CMV**) was performed to select the relevant metabolites (Anderssen et al., 2006) avoiding overfitting the models. This procedure was done following the methodology proposed by Westerhuis et al. (2008), which was also thoroughly described in the previous plasma metabolomic study performed on these lines (Zubiri-Gaitán et al., 2023). Briefly, the CMV performs an inner cross-validation (**CV**) to develop and optimize the models, and an outer CV to test the models' performance (Westerhuis et al., 2008). After exploratory analysis, a 7-fold inner CV and an 8-fold outer CV were used for the PLS-DA analysis, i.e., the samples were divided into 8 groups (8-fold outer CV), one group was set aside as a test set and the remaining samples (training set) were subjected to a 7-fold inner CV procedure to develop and optimize the model. For the PLS-H and PLS-L analyses, a 7-fold inner CV and a 5-fold outer CV were used.

A variable selection step was performed after the optimization of the model (inner CV) and before the prediction of the samples in the test set (outer CV). The metabolites were selected using the confidence interval of the variable's regression coefficients (**CI**) and the variable importance in projection value (**VIP**). First, metabolites that had a 95% CI containing the 0 were removed. Then, the relevant metabolites were selected according to their VIP value. To select variables based on the VIP value, the greater-than-one rule is normally used; however, higher or lower cutoff may be necessary to increase the variable selection performance (Chong and Jun, 2005). Therefore, in this study, several cutoff values were tested (0.8, 0.9, 1, 1.1, and 1.2), and their variable selection performance was analyzed based on the capacity of the new model to predict the samples in the test set.

The procedure was repeated 8 times for the PLS-DA and 5 for the PLS, until all the groups of the outer CV were set aside once. Additionally, 20 rounds of CMV were performed, changing the composition of the outer CV groups. Once all the PLS-DA and PLS models were adjusted, the metabolites considered as relevant in each approach (PLS-DA, PLS-H, and PLS-L) were those that were selected in more than 70% of the models.

The corresponding final models (PLS-DA, PLS-H, and PLS-L) were adjusted with the selected variables during a new CMV procedure. The classification ability of the PLS-DA was then evaluated using an average misclassification table, while the prediction ability of the PLS models (PLS-H and PLS-L) was evaluated using the Q^2 parameter. A permutation test was also performed as an additional validation method (Westerhuis et al., 2008), in which the values of the dependent variable (H and L classes for the PLS-DA or IMF content for the PLS) were permuted and the average misclassification table (PLS-DA) or Q^2 (PLS) of the permuted models were calculated.

The differences between lines of the metabolites selected during the PLS-DA analysis were estimated with a linear model that included the fixed effects of line and sex. Bayesian inference was applied (Blasco, 2001, 2017) using the R function *runRabbit* (Martínez-Álvaro et al., 2023). Bounded flat priors were assumed for all fixed effects and variances. The residual random effects were assumed to be a priori uncorrelated and multinormally distributed ($N(0, I\sigma^2_e)$). The marginal posterior distributions of the phenotypic differences between lines were obtained by Gibbs sampling, with a chain length of 60,000, a burn-in of 10,000, and a lag of 10. The parameters of the posterior distributions taken into consideration were the median of the difference between lines ($D_{H\text{-}L}$), the highest posterior density interval at 95% probability ($HPD_{95\%}$), and the probability of the difference being >0 when $D_{H\text{-}L} > 0$, or lower than zero when $D_{H\text{-}L} < 0$ (P_0) (Blasco, 2017). Finally, the difference between lines for each metabolite was expressed as units of SD of the metabolite, to give a better understanding of its magnitude.

The regression coefficients of the metabolites selected with the PLS-H and PLS-L analyses were estimated with a linear model that included the fixed effect of sex, and the IMF content as a covariate. The inferences were performed following the same methodology mentioned above. The parameters of the posterior distributions of the regression coefficients taken into consideration were the median (β), the $HPD_{95\%}$, and the probability of the coefficient being >0 when $\beta > 0$, or lower than zero when $\beta < 0$ (P_0).

Metabolic signature

All metabolites selected with the multivariate analyses were used to identify a metabolic signature composed of a small subset of metabolites with the ability to classify animals according to their genetic predisposition toward IMF deposition. A stepwise algorithm for compositional data was used for the selection of an optimal balance with the highest classification accuracy, using the *selbal* R package (Rivera-Pinto et al., 2018). A balance in compositional data analysis is a particular type of log-contrast between 2 groups of variables (Egozcue and Pawlowsky-Glahn, 2005; Rivera-Pinto et al., 2018), also known as isometric log-ratio (*ilr*). The numerator and denominator of such contrast are geometric means of multiple variables' abundances. The complete method is described in Rivera-Pinto et al. (2018). The optimal balance was established using a CV procedure implemented in the algorithm, as recommended by the authors (Rivera-Pinto et al., 2018). An 8-fold cross-validation was performed, which was in turn repeated 20 times. In each iteration, the algorithm stopped when the addition of a new metabolite to the balance did not improve the area under the ROC curve (Rivera-Pinto et al., 2018). In a second step, the selected balance was fitted in a logit regression to test its classification ability, using an 8-fold CV procedure, which

was repeated 20 times. The classification ability of the balance was finally evaluated using a misclassification table.

Results

A total of 711 compounds were detected with the 4 methodologies previously described (241 *positive-early*, 92 *positive-late*, 274 *negative*, and 104 *polar*). After the data processing, 633 metabolites were kept for further analysis: 226 from the *positive-early* dataset, 71 from the *positive-late*, 241 from the *negative*, and 95 from the *polar*, covering a wide range of biochemical compounds (Supplementary Table 2). Previous studies performed on these lines suggested that the biological mechanisms that led to greater or lower IMF content in each line are not entirely the same (Zubiri-Gaitán et al., 2022b, 2023). Hence, in this study, a 3-way approach was used to analyze the cecum metabolomics data: the PLS-DA to extract evidence regarding the pathways differentiating the lines, and the PLS-H and PLS-L to extract evidence regarding the specific pathways associated with IMF deposition within each line.

Multivariate analyses

PLS-DA analysis identified 142 metabolites during cross-model validation (CMV) that were relevant for the discrimination between lines (Supplementary Table 3). The final models adjusted with the relevant metabolites had a classification ability of 99% (Supplementary Table 4), while that estimated during the permutation test was around 50%, as expected when permuted data is used (i.e., no real differences exist between classes) and a proper cross-validation procedure is performed (Supplementary Table 5) (Westerhuis et al., 2008).

PLS-L analysis identified 107 metabolites that maximized the covariance with IMF (Supplementary Table 6), and PLS-H 156 metabolites (Supplementary Table 7), of which only 31 were important for both lines (Figure 1). The small overlap of relevant metabolites between analyses supports the hypothesis of some differences in the microbial metabolic pathways leading to higher or lower IMF content within each line. The Q^2 parameter of PLS models, estimated during CMV, evidenced a moderately good prediction accuracy of 57% for the L-line (Supplementary Table 8) and 61% for the H-line (Supplementary Table 9). These results were also validated by the corresponding permutation tests (Supplementary Tables 10 and S11).

Microbial metabolic pathways affected by selection

The classification of the relevant metabolites according to their chemical nature and the metabolic pathways in which they are involved was performed based on the information available in the Human Metabolome Database and the Kyoto Encyclopedia of Genes and Genomes database and is summarized in Figures 2 to 5.

Lipids were the most abundant metabolites detected in all 3 analyses, although they had a greater relative importance in the PLS-L, representing over 50% of the relevant metabolites. A more complex microbial metabolism was associated with IMF deposition in the H-line, as evidenced by the greater number of microbial pathways detected with the PLS-H analysis. The results from the PLS-DA showed that the most representative pathways differentiating between lines were those of purines and pyrimidines (i.e., nucleotides), secondary

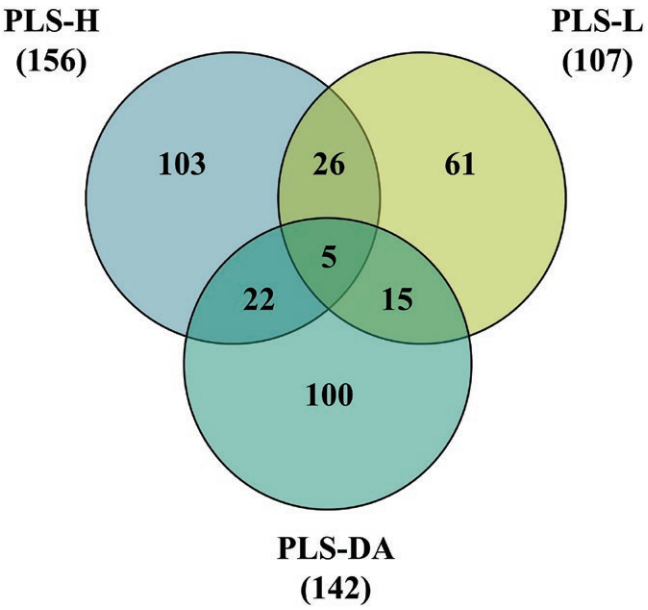

Figure 1. Venn diagram of relevant metabolites selected with PLS-DA (142 metabolites discriminating between lines), PLS-H (156 metabolites adjusting linearly to intramuscular fat content in animals from the high-IMF lines), and PLS-L (107 metabolites adjusting linearly to intramuscular fat content in animals from the low-IMF lines) analyses. PLS-DA: partial least square—discriminant analysis; PLS-H: linear partial least square performed only with animals from the high-IMF line; PLS-L: linear partial least square performed only with animals from the low-IMF line.

bile acids, and of several amino acids, from which aromatic amino acids (**AAA**) and BCAA stand out. Additionally, many relevant metabolites were food components (i.e., xenobiotics), dicarboxylate fatty acids, dipeptides, acyl carnitines, gamma-glutamyl amino acids, and phosphatidylcholines (Figure 3). The results from the PLS-L (Figure 4) and PLS-H (Figure 5) suggested that the lysophospholipids content in the cecum is related to the IMF content in both lines. However, the cecum content of nucleotides' metabolites, secondary bile acids, and xenobiotics seemed more closely related to IMF content in the H-line, while that of the long-chain fatty acids seemed more closely related to IMF content in the L-line.

The PLS-DA identified greater abundance in the cecum of the H-line of the AAA tryptophan (0.76 SD, $P_0 = 1$) and tyrosine (1.16 SD, $P_0 = 1$), together with tryptophan's degradation products indole (1.02 SD, $P_0 = 1$) and indoleacetate (0.49 SD, $P_0 = 0.96$), while the 5-hydroxyindoleacetate (5-HIAA) was greater in the L-line (-0.54 SD, $P_0 = 0.97$). Tryptophan metabolism was also identified in the PLS-H, but not in the PLS-L. The previously mentioned indoleacetate was positively related to IMF content in the H-line ($\beta > 0$; $P_0 = 1$), together with tryptophol ($\beta > 0$; $P_0 = 0.99$), kynurenine ($\beta > 0$; $P_0 = 0.99$) and anthranilate ($\beta > 0$; $P_0 = 0.97$).

The metabolism of BCAA (valine, leucine, and isoleucine) was also affected by selection, evidencing differences between lines and linear relationship with IMF in both lines. N-acetylisoleucine was more abundant in the cecum of the L-line (–0.51 SD, $P_0 = 0.96$), and it was also negatively related to the IMF content in the mentioned line ($\beta < 0$; $P_0 = 0.99$). Isobutyrylcarnitine was greater in the H-line (0.37 SD, $P_0 = 0.91$) and, even though there was no evidence of differences between lines, isovalerylglycine was negatively associated with IMF in the L-line ($\beta < 0$; $P_0 = 0.98$). Additionally,

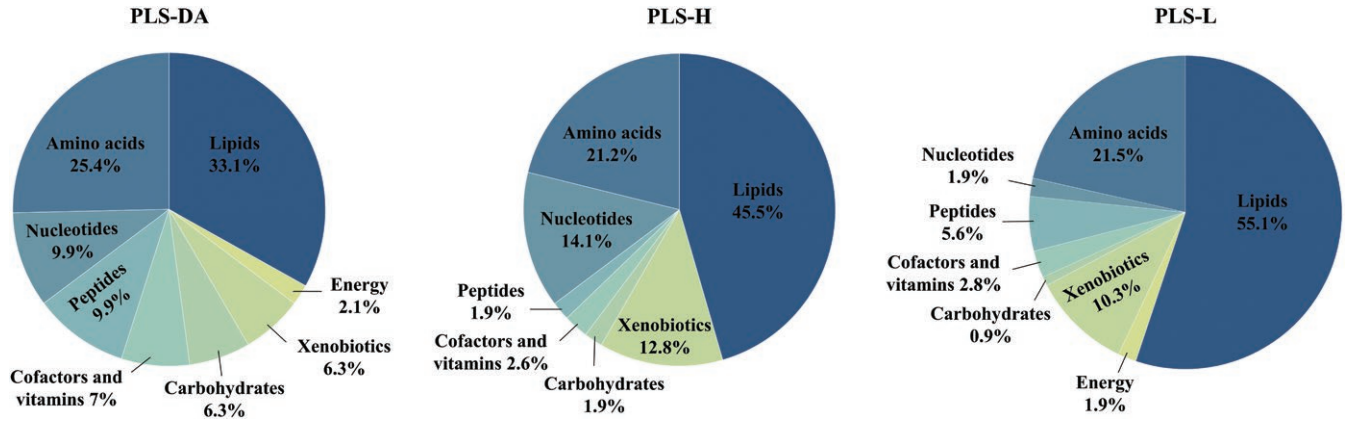

Figure 2. Classification of relevant metabolites selected in the PLS-DA (142 metabolites), PLS-H (156 metabolites), and PLS-L (107 metabolites) models according to their chemical nature. PLS-DA: partial least square—discriminant analysis; PLS-H: linear partial least square performed only with animals from the high-IMF line; PLS-L: linear partial least square performed only with animals from the low-IMF line.

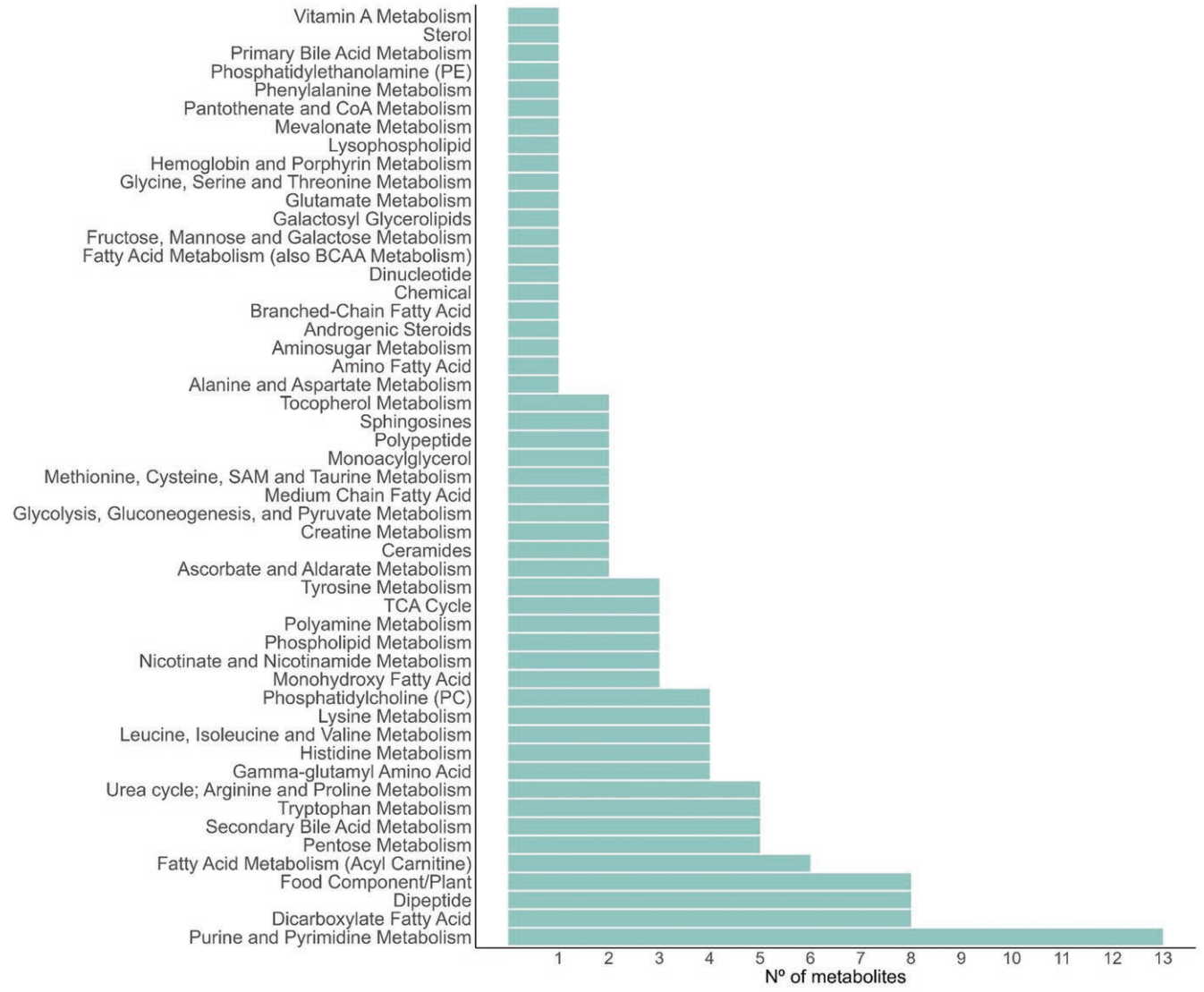

Figure 3. Classification of the 142 relevant metabolites selected in the partial least square—discriminant analysis (PLS-DA) model according to the metabolic pathways in which they are involved.

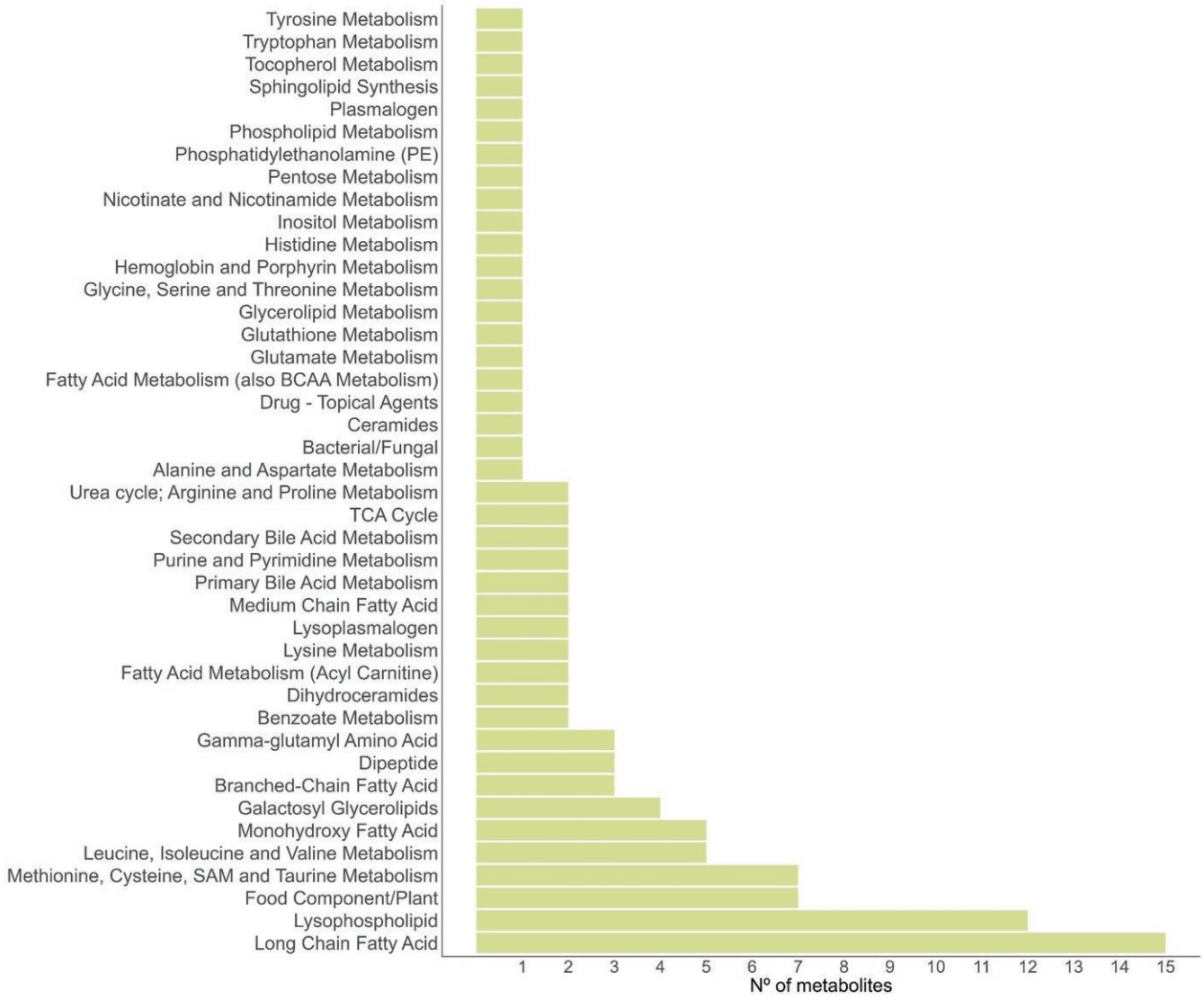

Figure 4. Classification of the 107 relevant metabolites selected in the partial least square model adjusted using only animals from the low-IMF line (PLS-L) according to the metabolic pathways in which they are involved.

glycine, an amino acid whose availability has been shown to be related to the BCAA (White et al., 2016), was also negatively associated with IMF in the L-line ($\beta < 0$; $P_0 = 0.88$).

Also related to the metabolism of proteins and amino acids, most of the dipeptides and polypeptides found were more abundant in the cecum of the H-line (from 0.41 to 0.89 SD, all $P_0 \geq 0.94$), whereas the gamma-glutamyl amino acids were more abundant in the cecum of the L-line (from −0.55 to −0.62 SD, all $P_0 \geq 0.97$). The gamma-glutamyl amino acids were also found in the PLS-H and PLS-L, evidencing a negative relationship with the IMF content ($\beta < 0$; all $P_0 \geq 0.93$). Additionally, 2-hydroxybutyrate, a metabolite related to glutathione metabolism and consequently to gamma-glutamyl amino acids, was positively related to IMF in both H and L-lines ($\beta > 0$; $P_0 = 1$ in the H-line and $P_0 = 0.94$ in the L-line).

The cecum of the L-line showed greater abundance of numerous lipids, including mevalonate (−0.50 SD, $P_0 = 0.96$), involved in the metabolism of cholesterol, 4-cholesten-3-one (−0.42 SD, $P_0 = 0.93$), a cholesterol derivative formed in the gastrointestinal tract, sphingosines, phosphatidylethanolamines, phosphatidylcholines, and other metabolites related to phospholipid metabolism (from −0.36 to −0.72 SD, all $P_0 \geq 0.89$). Several secondary bile acids were greater in the L-line (from −0.19 to −0.52 SD, all $P_0 \geq 0.76$), similar to what was found in the plasma of these lines (Zubiri-Gaitán et al., 2023), with the only exception of the 7-ketodeoxycholate, which was greater in the H-line (0.82 SD, $P_0 = 1$). Additionally, numerous secondary bile acids metabolites were positively related to the IMF content only in the H-line ($\beta > 0$; all $P_0 \geq 0.95$).

The lysophospholipids, which were not relevant to the discrimination between lines, were instead some of the most representative metabolites related to the IMF content in both lines ($\beta > 0$; all $P_0 \geq 0.94$). Similarly, while there were no differences between lines neither in long-chain (**LC**) saturated fatty acids (LC-SFA) nor branched-chain fatty acids (**BCFA**), they were found to be positively related to IMF but only in the L-line ($\beta > 0$; all $P_0 \geq 0.93$).

Finally, the PLS-DA identified greater abundance in the cecum of the H-line of purines and pyrimidines metabolites, including dinucleotides, nucleosides, and nucleotides (from 0.54 to 1.07 SD, all $P_0 \geq 0.97$). Hypoxanthine, a product of purine catabolism, was also greater in the H-line (0.56 SD, P_0

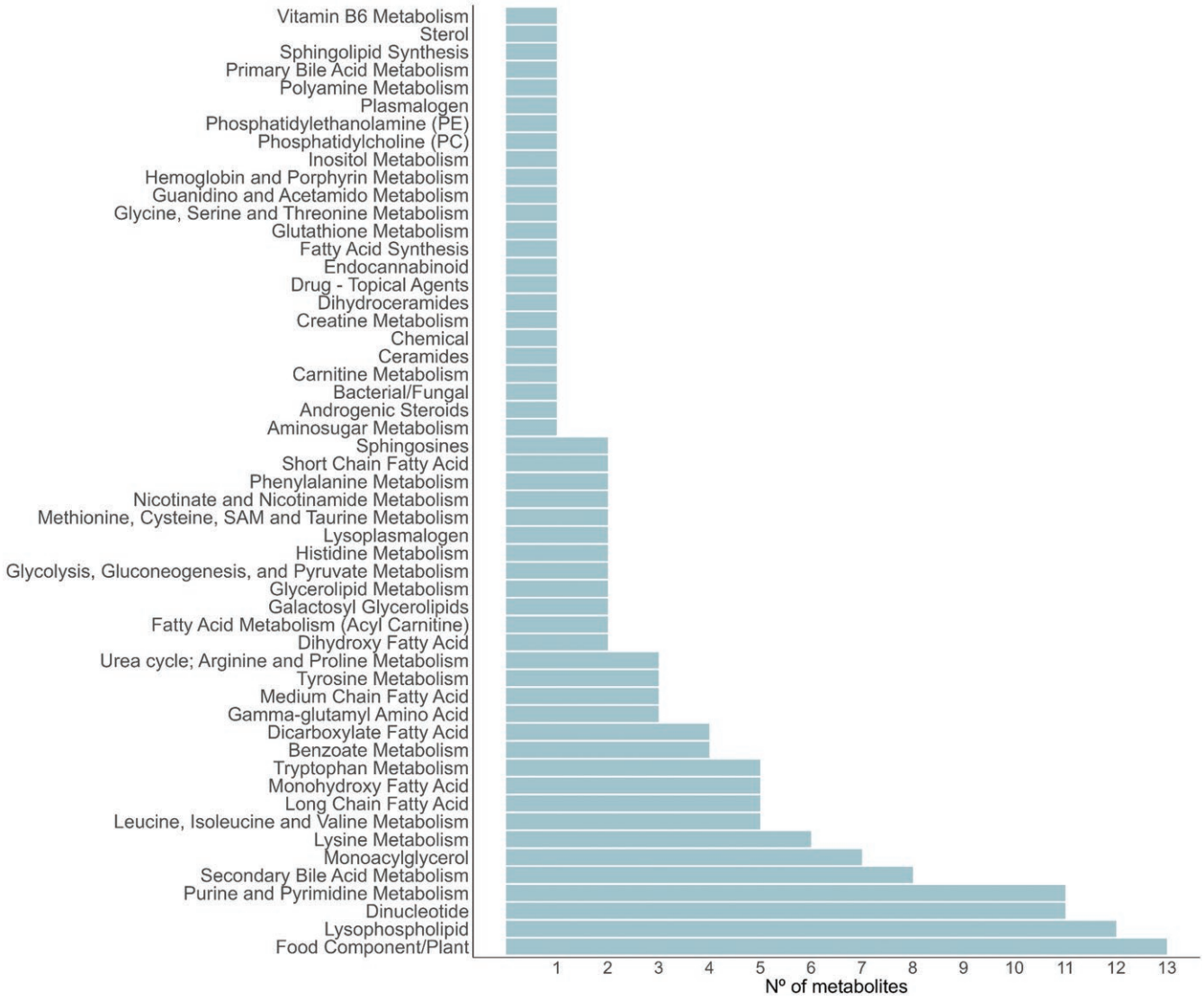

Figure 5. Classification of the 156 relevant metabolites selected in the partial least square model adjusted using only animals from the high-IMF line (PLS-H) according to the metabolic pathways in which they are involved.

= 0.98), while other products were greater in the L-line like urate (-0.45 SD, P_0 = 0.95), allantoin (-0.58 SD, P_0 = 0.98), and dAMP (-0.40 SD, P_0 = 0.92). Dinucleotides, nucleosides, and nucleotides were also relevant results of the PLS-H analysis, and they all had a positive relationship with IMF ($\beta > 0$; all $P_0 \geq 0.94$).

Metabolic signature

The detection of a metabolic signature, composed of a small subset of metabolites with high classification accuracy, might be interesting to identify the main microbial pathways related to IMF deposition. Hence, once the main pathways associated with IMF deposition were identified, a stepwise algorithm was used to select an optimal balance, as described in the methodology section. The balance with the highest classification accuracy was composed of 4 metabolites, 2 in the numerator (guanidinoacetate and glycodeoxycholate) and 2 in the denominator (glycylisoleucine and 7-ketodeoxycholate). The metabolites in the numerator were greater in the L-line (guanidinoacetate: −1.03 SD, P_0 = 1; glycodeoxycholate: −0.52 SD, P_0 = 0.97), while those in the denominator were greater in the H-line (glycylisoleucine: 0.89 SD, P_0 = 1; 7-ketodeoxycholate: 0.82 SD, P_0 = 1). The computed value of the balance (or *ilr*) for each individual is shown in Supplementary Table 12, and their distribution is shown in Figure 6. The logit model adjusted with the selected balance showed an outstanding classification ability of 88% (Supplementary Table 13).

Discussion

Amino acids and peptides

Amino acid metabolic pathways are among the most affected by the microbiota, affecting the metabolomic profile of the gastrointestinal tract and of other tissues (Zarei et al., 2022). The greater cecum abundance of tryptophan and tyrosine found in the H-line agrees with the greater abundance of the *tyrC* gene, involved in their biosynthesis, found in this line in the previous metagenomic analysis (Martínez-Álvaro et al., 2021). Indole and indoleacetate, both greater in the H-line, are tryptophan degradation products produced by bacteria (Roager and Licht, 2018), while the 5-HIAA, greater in the L-line, is the excretion

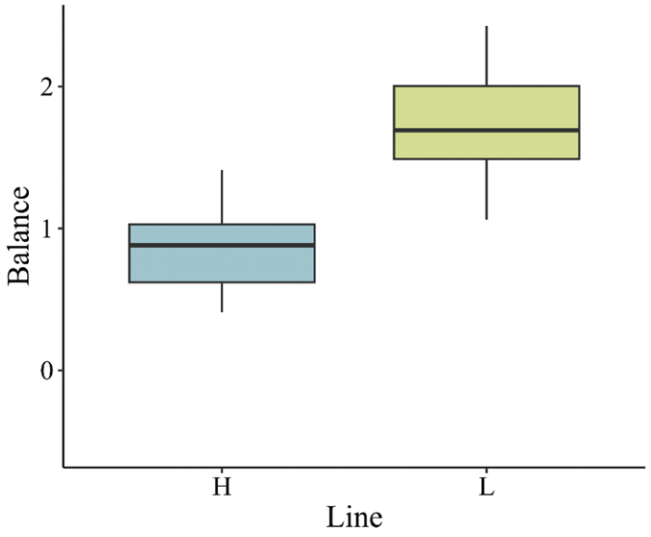

Figure 6. Distribution of the isometric log-ratio (*ilr*) balance according to the genetic line (high- or low-IMF line). The balance was composed of 2 metabolites in the numerator (guanidinoacetate and glycodeoxycholate) and 2 in the denominator (glycylisoleucine and 7-ketodeoxycholate). The logit model adjusted with the selected balance showed an outstanding classification ability of 88%.

product of serotonin (Le Floc'h et al., 2011). Serotonin is synthesized from tryptophan, and these results could indicate a difference between lines in the metabolic fate of this essential amino acid. Additionally, a previous microbiome analysis performed on these lines showed that Lactobacillus, a bacteria that plays an important role in the detoxification of indole compounds (Nowak et al., 2008), was less abundant in the cecum of the H-line (Martínez-Álvaro et al., 2024), which could also explain the greater abundance of these metabolites in the mentioned line. The metabolism of tryptophan was also relevant in determining the IMF content in the H-line. Indoleacetate and tryptophol, metabolites from the microbial indole pathway, and kynurenine and anthranilate, from the host kynurenine pathway, were positively related to IMF. Both pathways have been shown to be altered in obesity in humans, most likely because of their role in the inflammatory processes related (Cussotto et al., 2020). The kynurenine pathway is activated by pro-inflammatory cytokines and has therefore been positively associated with obesity; however, a negative association has been found with the indole metabolites (Bansal et al., 2010; Wlodarska et al., 2017; Cussotto et al., 2020). Plasma metabolites from both pathways, including the kynurenine, were also positively associated with IMF in these lines (Zubiri-Gaitán et al., 2023), suggesting that both the host and its microbiome play an important role in the metabolism of tryptophan in relation to IMF deposition.

BCAA metabolism is strongly associated with obesity and insulin resistance in humans (Siddik and Shin, 2019; Vanweert et al., 2022). The circulating levels of BCAA have been positively associated with obesity (Newgard et al., 2009; Kim et al., 2010; Siddik and Shin, 2019) and with IMF content in pigs (Taniguchi et al., 2020) and cattle (Connolly et al., 2019). Current evidence suggests that these relationships are the result of the action of multiple factors related to their synthesis and catabolism, rather than by differences in their intake (Tai et al., 2010; Newgard, 2012), in which a greater production and lower catabolism of BCAA by the intestinal microbiota seems to be one potential factor contributing to the greater fat deposition (Ridaura et al., 2013). In these divergent rabbit lines, results from the genomic (Sosa-Madrid et al., 2020), metagenomic (Martínez-Álvaro et al., 2021), plasma metabolomic (Zubiri-Gaitán et al., 2023), and cecal metabolomic analyses confirmed the strong and complex relationship between the BCAA metabolism, both from the host and its microbiota, with fat deposition in both lines. It has been shown that isoleucine upregulates the intestinal glucose transporters (Zhang et al., 2017), enhancing glucose absorption and utilization, suggesting that the negative relationship found between IMF and N-acetylisoleucine in both the PLS-DA and PLS-L analyses might be related to the glucose utilization and that this mechanism may be more important in the L-line. The circulating levels of short-chain acylcarnitines, related to the metabolism of BCAA, have been positively associated with fat deposition in humans (Libert et al., 2018), which was also observed in the plasma of these lines (Zubiri-Gaitán et al., 2023). However, in this study, the PLS-DA did not identify a clear signature that discriminated between the lines, and the greater abundance of isobutyrylcarnitine found in the cecum of the H-line may be associated with the greater plasma abundance found (Zubiri-Gaitán et al., 2023). In humans, the glycine and isovalerylglycine concentration in blood (Tai et al., 2010) and urine (Newgard et al., 2009) have been negatively associated with obesity and insulin resistance, similar to what was observed in both the cecum and plasma (Zubiri-Gaitán et al., 2023) of the L-line. A study performed in genetically obese and lean rats showed that the rise in circulating BCAA observed in obesity is responsible for the lower circulating levels of glycine commonly observed, and that this limited availability of glycine can be responsible for the lower formation of acylglycines (White et al., 2016).

Glutathione is an essential antioxidant in mammalian cells, whose intracellular concentrations are maintained by the activity of the γ-glutamyltransferase (GGT) enzyme. The GGT catalyzes the transfer of the gamma-glutamyl group from glutathione to amino acids, thus forming gamma-glutamyl amino acids (Mitrić and Castellano, 2023). Serum GGT levels in humans have been positively associated with fat deposition, type 2 diabetes, and metabolic syndrome (Rantala et al., 2000; Duk et al., 2004; Coku and Shkembi, 2018; Sheng et al., 2022), although the relationship between serum GGT and gamma-glutamyl amino acids has not been established. A recent study performed in mice suggested that the circulating levels of gamma-glutamyl amino acids are impacted by interactions between microbes and dietary fibers (Murga-Garrido et al., 2021), evidencing a complex co-metabolism between the host and its microbiota. On the other hand, the 2-hydroxybutyrate is also related to glutathione metabolism, as it is a byproduct of its synthesis, and its urinary excretion has been proposed as a marker for chronic shifts in the rate of glutathione synthesis. In these lines, the negative relationship between IMF and gamma-glutamyl amino acids, and the positive relationship between IMF and 2-hydroxibutyrate, found both in plasma (Zubiri-Gaitán et al., 2023) and cecum, indicate an interesting and complex co-metabolism that would benefit from further studies to unravel its role in fat deposition.

Lipids

Lipids were the most abundant metabolites detected in all 3 multivariate analyses and the results from the PLS-H and

PLS-L analyses showed that their relationship with IMF was positive. As mentioned in the previous section, lipids had a greater relative importance in the PLS-L while, as evidenced by the results discussed so far, a more complex microbiota metabolism might be related to IMF deposition in the H-line.

The intestinal absorption of triglycerides and fatty acids has been shown to be a significant determinant of their plasma levels (Fujisaka et al., 2018). In these lines, the greater amount of bile acids found in both plasma and cecum of the L-line, essential for lipid digestion and absorption in the gastrointestinal tract (Di Ciaula et al., 2017; Nelson and Cox, 2021a), together with its greater plasma abundance of triglycerides, cholesterol and non-esterified fatty acids, among others, (Martínez-Álvaro et al., 2018b; Zubiri-Gaitán et al., 2022a, 2023) supports this theory. However, despite this hypothesized greater intestinal absorption, the animals from the L-line appear to have a lower capacity for uptake, re-esterification, and storage due to their genetic predisposition (Zubiri-Gaitán et al., 2023). The former is probably also the reason why most of these secondary bile acids did not show a linear relationship with IMF in the L-line, as opposed to the H-line.

Microbial lipids metabolism in cecotrophic animals like rabbit is more important than in other hindgut fermenters because they recycle an important part of the unabsorbed nutrients through cecotrophy. Particularly, the microbial fermentation of lipids in the cecum of rabbits yields a distinctive fatty acid profile, characterized by an increased proportion of BCFA and SFA (especially those with more than 12 carbon atoms) (Leiber et al., 2008). Because of the ingestion of the cecotrophes, these fatty acids can reach the duodenum and be absorbed into the bloodstream. The relationship between LC-SFA and BCFA with IMF, detected only in the PLS-L analysis, suggests that a greater microbial biohydrogenation of lipids might be related to a greater IMF deposition in the L-line. On the other hand, the lysophospholipids were related to IMF deposition in both lines. Cecal content of lysophospholipids has been shown to be altered in chickens with obese and lean phenotypes, although their mechanisms were not entirely clear (Liu et al., 2022). The intestinal content of lysophospholipids is the result of the phospholipids' hydrolysis, which is in turn necessary for lipid absorption (Beil and Grundy, 1980). The absorption of these lysophospholipids has also been related to increased inflammation, leading to an increased risk of obesity in humans (Hui, 2016). These results point out that, independently of the genetic line, the intestinal metabolism of phospholipids is relevant for the deposition of intramuscular fat, although further studies are necessary to elucidate the mechanisms.

Nucleotides

The nucleotides' metabolites were some of the most relevant in discriminating between lines and also explaining the IMF content in the H-line, but not in the L-line. While urate and allantoin were greater in the L-line, hypoxanthine was greater in the H-line. Urate is the product of purine catabolism, while allantoin is the oxidation product of urate (Rudolph, 1994; Nelson and Cox, 2021b). Those metabolites, together with xanthine and hypoxanthine, are called purine derivatives (**PD**), and they originate from the ingested purine bases or from the turnover of nucleic acids (Nelson and Cox, 2021b). The catabolism of nucleic acids occurs mostly in the intestinal mucosa, where they are rapidly degraded to their oxidized derivatives by the high xanthine oxidase enzyme (Balcells et al., 1998). The former catalyzes the oxidation from hypoxanthine to xanthine, and from xanthine to urate. In this experiment, while the urate and the allantoin were greater in the L-line, the hypoxanthine was greater in the H-line, which could suggest a difference between the lines in the activity of the mentioned enzyme.

PD are also important because of their use as a biological marker of the microbial nitrogen recycling in ruminants and cecotrophic animals like rabbit. These animals recycle most of the microbial protein produced during the fermentation; in the case of rabbits through cecotrophy (Hörnicke, 1981). The purine base content in the cecotrophes is considered to be of the microbial origin (Balcells et al., 1998), and is used as a marker of microbial concentrations (Blas and Wiseman, 2020). In turn, the urinary PD excretion is used as a marker to estimate the microbial protein synthesis, its intake from cecotrophy, and the consequent microbial nitrogen recycling (Balcells et al., 1998; Belenguer et al., 2002). No evidence was found in the literature regarding this relationship with the PD cecum content, although it has been estimated that around 40% of net microbial synthesis is lost through feces (Balcells et al., 1998). The modification of cecal fermentation through changes in the diet has been used to improve the microbial contribution to the rabbits' protein nutrition (Belenguer et al., 2002). One study performed in lambs showed that diets with greater rumen undegradable protein to rumen degradable protein ratio led to a greater urinary PD excretion and lower carcass fat content, which was suggested to be related to greater nitrogen utilization and energy efficiencies (Valizadeh et al., 2021). Since these lines are fed the same diet, and if the relationship between urinary and cecum PD is maintained, the differences found may suggest changes in their fermentation activity caused by a different microbiome composition. These results suggest that this pathway could be of interest for further investigation.

Metabolic signature

The application of supervised multivariate methods like PLS and PLS-DA is useful to identify all variables with the ability to predict a trait of interest, even if they contain redundant information. Conversely, based on the complex interactions between metabolites and their pathways, computing a compositional balance can be the optimal solution to find a metabolic signature with good prediction accuracy and biological sense for IMF deposition, which could be then investigated in other species.

The metabolites finally selected to conform the balance, or isometric log-ratio (*ilr*), were 2 secondary bile acids (7-ketodeoxycholate and glycodeoxycholate), one dipeptide (glycylisoleucine), and one metabolite from the creatine metabolism (guanidinoacetate). As mentioned in the previous section, glycodeoxycholate and guanidinoacetate were greater in the L-line, and they made up the numerator, while 7-ketodeoxycholate and glycylisoleucine were greater in the H-line and they made up the denominator. Secondary bile acids are very important for lipid absorption in the gastrointestinal tract (Di Ciaula et al., 2017; Nelson and Cox, 2021a), and the glycylisoleucine and guanidinoacetate are both related to the protein metabolism. Both are very important

pathways in fat deposition, and in these lines, they have been identified as some of the most relevant pathways based on the metabolomics analysis of the cecum, but also of the plasma (Zubiri-Gaitán et al., 2023).

Based on these results, it can be suggested that the interaction between the lipids' absorption and the metabolism of the proteins from the diet is a potential main driver of the microbiome activity influencing the trait under selection. Even though this result needs to be validated, it constitutes a very promising proposal to evaluate the microbial activity based on its ability to classify animals according to their genetic predisposition toward IMF deposition.

Conclusions

In this study, the use of 2 lines divergently selected for IMF content allowed us to study the genetically determined microbial metabolic pathways associated with IMF deposition, independently from the environmental factors. The comprehensive analysis of the results showed that the most relevant microbial pathways differentiating the lines were those of amino acids (aromatic, branched-chain, and gamma-glutamyl amino acids), lipids (especially secondary bile acids), and nucleotides (purine metabolism). The microbial metabolic pathways related to IMF deposition within each line showed that lipids' metabolism had a greater relative importance in the L line, while a more complex microbial metabolism was associated with IMF deposition in the H-line, as evidenced by the greater amount of related microbial pathways detected. To the authors' knowledge, this is the first study that identifies a metabolic signature of the microbial metabolism influencing IMF deposition, which was composed of 2 secondary bile acids and 2 products of proteins' metabolism and had an outstanding classification ability of 88%.

Supplementary Data

Supplementary data are available at *Journal of Animal Science* online.

Data availability statement

None of the data were deposited in an official repository. The datasets analyzed during the current study are available from the corresponding author upon reasonable request.

Declaration of generative AI and AI-assisted technologies in the writing process

The authors did not use any artificial intelligence-assisted technologies in the writing process.

Acknowledgments

The authors thank Federico Prado for his technical assistance, and María Antonia Santacreu, Noelia Ibañez-Escriche, and Cristina Casto-Rebollo for their assistance in the sampling.

A preprint version of this research article has been published in Research Square: https://doi.org/10.21203/rs.3.rs-3852991/v1. This study was funded by the Spanish Ministry of Science and Innovation, project number PID2020-115558GB-C21, and by the Conselleria for Innovation, Universities, Science and Digital Society, project number AICO/2020/349. M.M-A. thanks the Spanish Ministry of Science and Innovation for a Ramon y Cajal grant (RYC2021-032618-I) funded by MCIN/AEI/10.13039/501100011033 and the European Union Next Generation EU/PRTR.

Conflict of interest statement

The authors declare that they have no competing financial interests or personal relationships that could have influenced the work reported in this paper.

Author contributions

Agostina Zubiri-Gaitán (Data curation, Formal analysis, Investigation, Methodology, Writing—original draft), Marina Martínez Álvaro (Investigation, Methodology, Supervision, Writing—review & editing), Agustin Blasco (Conceptualization, Funding acquisition, Project administration, Resources, Supervision, Writing—review & editing), and Pilar Hernandez (Conceptualization, Funding acquisition, Investigation, Methodology, Supervision, Writing—review & editing)

Literature Cited

Alseekh, S., A. Aharoni, Y. Brotman, K. Contrepois, J. D'Auria, J. Ewald, J. C. Ewald, P. D. Fraser, P. Giavalisco, R. D. Hall, et al. 2021. Mass spectrometry-based metabolomics: a guide for annotation, quantification and best reporting practices. Nat. Methods. 18:747–756. doi:10.1038/s41592-021-01197-1

Anderssen, E., K. Dyrstad, F. Westad, and H. Martens. 2006. Reducing over-optimism in variable selection by cross-model validation. Chemometr. Intell. Lab. Syst. 84:69–74. doi:10.1016/j.chemolab.2006.04.021

Bäckhed, F., H. Ding, T. Wang, L. V. Hooper, Y. K. Gou, A. Nagy, C. F. Semenkovich, and J. I. Gordon. 2004. The gut microbiota as an environmental factor that regulates fat storage. Proc. Natl. Acad. Sci. U.S.A. 101:15718–15723. doi:10.1073/pnas.0407076101

Balcells, J., J. M. Ganuza, J. F. Pérez, S. M. Martín-Orúe, and M. González Ronquillo. 1998. Urinary excretion of purine derivatives as an index of microbial-nitrogen intake in growing rabbits. Br. J. Nutr. 79:373–380. doi:10.1079/bjn19980062

Bansal, T., R. C. Alaniz, T. K. Wood, and A. Jayaraman. 2010. The bacterial signal indole increases epithelial-cell tight-junction resistance and attenuates indicators of inflammation. Proc. Natl. Acad. Sci. U.S.A. 107:228–233. doi:10.1073/pnas.0906112107

Beil, F. U., and S. M. Grundy. 1980. Studies on plasma lipoproteins during absorption of exogenous lecithin in man. J. Lipid Res. 21:525–536. doi:10.1016/s0022-2275(20)42223-0

Belenguer, A., J. Balcells, M. Fondevila, and C. Torre. 2002. Caecotrophes intake in growing rabbits estimated either from urinary excretion of purine derivatives or from direct measurement using animals provided with a neck collar: Effect of type and level of dietary carbohydrate. Anim. Sci. 74:135–144. doi:10.1017/s1357729800052309

Blas C. and J. Wiseman, editors. 2020. Nutrition of the rabbit. 3rd ed. Wallingford (UK): CABI.

Blasco, A. 2001. The Bayesian controversy in animal breeding. J. Anim. Sci. 79:2023–2046. doi:10.2527/2001.7982023x

Blasco, A. 2017. Bayesian data analysis for animal scientists: the basics. 1st ed. Switzerland: Springer Cham.

Bonder, M. J., A. Kurilshikov, E. F. Tigchelaar, Z. Mujagic, F. Imhann, A. V. Vila, P. Deelen, T. Vatanen, M. Schirmer, S. P. Smeekens, et al. 2016. The effect of host genetics on the gut microbiome. Nat. Genet. 48:1407–1412. doi:10.1038/ng.3663

Cani, P. D., R. Bibiloni, C. Knauf, A. Waget, A. M. Neyrinck, N. M. Delzenne, and R. Burcelin. 2008. Changes in gut microbiota control metabolic endotoxemia-induced inflammation in high-fat diet-induced obesity and diabetes in mice. Diabetes. 57:1470–1481. doi:10.2337/db07-1403

Chong, I. G., and C. H. Jun. 2005. Performance of some variable selection methods when multicollinearity is present. Chemom. Intell. Lab. Syst. 78:103–112. doi:10.1016/j.chemolab.2004.12.011

Clarke, G., R. M. Stilling, P. J. Kennedy, C. Stanton, J. F. Cryan, and T. G. Dinan. 2014. Minireview: Gut microbiota: The neglected endocrine organ. Mol. Endocrinol. 28:1221–1238. doi:10.1210/me.2014-1108

Coku, V., and X. Shkembi. 2018. Serum Gamma-glutamyltransferase and Obesity: is there a Link? Med. Arch. 72:112–115. doi:10.5455/medarh.2017.72.112-115

Connolly, S., A. Dona, L. Wilkinson-White, D. Hamblin, M. D'Occhio, and L. A. González. 2019. Relationship of the blood metabolome to subsequent carcass traits at slaughter in feedlot Wagyu crossbred steers. Sci. Rep. 9:1–11. doi:10.1038/s41598-019-51655-2

Cussotto, S., I. Delgado, A. Anesi, S. Dexpert, A. Aubert, C. Beau, D. Forestier, P. Ledaguenel, E. Magne, F. Mattivi, et al. 2020. Tryptophan metabolic pathways are altered in obesity and are associated with systemic inflammation. Front. Immunol. 11:1–7. doi:10.3389/fimmu.2020.00557

Di Ciaula, A., G. Garruti, R. L. Baccetto, E. Molina-Molina, L. Bonfrate, D. Q. H. Wang, and P. Portincasa. 2017. Bile acid physiology. Ann. Hepatol. 16:s4–s14. doi:10.5604/01.3001.0010.5493

Duk, H. L., K. Silventoinen, D. R. Jacobs, P. Jousilahti, and J. Tuomileto. 2004. γ-glutamyltransferase, obesity, and the risk of type 2 diabetes: Observational cohort study among 20,158 middle-aged men and women. J. Clin. Endocrinol. Metab. 89:5410–5414. doi:10.1210/jc.2004-0505

Egozcue, J. J., and V. Pawlowsky-Glahn. 2005. Groups of Parts and Their Balances in Compositional Data Analysis. Math. Geol. 37:795–828. doi:10.1007/s11004-005-7381-9

Fang, S., X. Xiong, Y. Su, L. Huang, and C. Chen. 2017. 16S rRNA gene-based association study identified microbial taxa associated with pork intramuscular fat content in feces and cecum lumen. BMC Microbiol. 17:1–9. doi:10.1186/s12866-017-1055-x

Fiehn, O. 2002. Metabolomics - The link between genotypes and phenotypes. Plant Mol. Biol. 48:155–171. doi:10.1023/A:1013713905833

Frank, D., S. T. Joo, and R. Warner. 2016. Consumer acceptability of intramuscular fat. Korean J. Food Sci. Anim. Resour. 36:699–708. doi:10.5851/kosfa.2016.36.6.699

Fricker, A. M., D. Podlesny, and W. F. Fricke. 2019. What is new and relevant for sequencing-based microbiome research? A mini-review. J. Adv. Res. 19:105–112. doi:10.1016/j.jare.2019.03.006

Fujisaka, S., J. Avila-Pacheco, M. Soto, A. Kostic, J. M. Dreyfuss, H. Pan, S. Ussar, E. Altindis, N. Li, L. Bry, et al. 2018. Diet, genetics, and the gut microbiome drive dynamic changes in plasma metabolites. Cell Rep. 22:3072–3086. doi:10.1016/j.celrep.2018.02.060

Greenacre, M. 2018. Compositional data analysis in practice. 1st ed. London (UK): Chapman and Hall/CRC.

Greenacre, M., M. Martínez-Álvaro, and A. Blasco. 2021. Compositional data analysis of microbiome and any-omics datasets: a validation of the additive logratio transformation. Front. Microbiol. 12:1–11. doi:10.3389/fmicb.2021.727398

Hörnicke, H. 1981. Utilization of caecal digesta by caecotrophy (soft faeces ingestion) in the rabbit. Livest. Prod. Sci. 8:361–366. doi:10.1016/0301-6226(81)90054-3

Hui, D. Y. 2016. Intestinal phospholipid and lysophospholipid metabolism in cardiometabolic disease. Curr. Opin Lipidol 27:507–512. doi:10.1097/MOL.0000000000000334

Jing, Y., Y. Yuan, M. Monson, P. Wang, F. Mu, Q. Zhang, W. Na, K. Zhang, Y. Wang, L. Leng, et al. 2022. Multi-Omics Association reveals the effects of intestinal microbiome–host interactions on fat deposition in broilers. Front. Microbiol. 12:1–18. doi:10.3389/fmicb.2021.815538

Kapoore, R. V., and S. Vaidyanathan. 2016. Towards quantitative mass spectrometry-based metabolomics in microbial and mammalian systems. Philos. Trans. R. Soc. A Math. Phys. Eng. Sci. 374:20150363. doi:10.1098/rsta.2015.0363

Kim, J. Y., J. Y. Park, O. Y. Kim, B. M. Ham, H. -J. Kim, D. Y. Kwon, Y. Jang, and J. H. Lee. 2010. Metabolic profiling of plasma in overweight/obese and lean men using ultra performance liquid chromatography and Q-TOF mass spectrometry (UPLC– Q-TOF MS). J. Proteome Res. 9:4368–4375. doi:10.1021/pr100101p

Krause, T. R., J. M. Lourenco, C. B. Welch, M. J. Rothrock, T. R. Callaway, and T. D. Pringle. 2020. The relationship between the rumen microbiome and carcass merit in Angus steers. J. Anim. Sci. 98:1–12. doi:10.1093/JAS/SKAA287

Kucheryavskiy, S. 2020. mdatools – R package for chemometrics. Chemometr. Intell. Lab. Syst. 198:103937. doi:10.1016/j.chemolab.2020.103937

Larraufie, P., C. Martin-Gallausiaux, N. Lapaque, J. Dore, F. M. Gribble, F. Reimann, and H. M. Blottiere. 2018. SCFAs strongly stimulate PYY production in human enteroendocrine cells. Sci. Rep. 8:74. doi:10.1038/s41598-017-18259-0

Le Floc'h, N., W. Otten, and E. Merlot. 2011. Tryptophan metabolism, from nutrition to potential therapeutic applications. Amino Acids 41:1195–1205. doi:10.1007/s00726-010-0752-7

Leiber, F., J. S. Meier, B. Burger, H. -R. Wettstein, M. Kreuzer, J. -M. Hatt, and M. Clauss. 2008. Significance of coprophagy for the fatty acid profile in body tissues of rabbits fed different diets. Lipids. 43:853–865. doi:10.1007/s11745-008-3210-5

Libert, D. M., A. S. Nowacki, and M. R. Natowicz. 2018. Metabolomic analysis of obesity, metabolic syndrome, and type 2 diabetes: amino acid and acylcarnitine levels change along a spectrum of metabolic wellness. PeerJ. 6:e5410. doi:10.7717/peerj.5410

Lim, Y. Y., Y. S. Lee, and D. S. Q. Ooi. 2020. Engineering the gut microbiome for treatment of obesity: a review of current understanding and progress. Biotechnol. J. 15:1–10. doi:10.1002/biot.202000013

Liu, J., J. Wang, Y. Zhou, H. Han, W. Liu, D. Li, F. Li, D. Cao, and Q. Lei. 2022. Integrated omics analysis reveals differences in gut microbiota and gut-host metabolite profiles between obese and lean chickens. Poult. Sci. 101:102165. doi:10.1016/j.psj.2022.102165

Lopera-Maya, E. A., A. Kurilshikov, A. van der Graaf, S. Hu, S. Andreu-Sánchez, L. Chen, A. V. Vila, R. Gacesa, T. Sinha, V. Collij, et al. 2022. Effect of host genetics on the gut microbiome in 7,738 participants of the Dutch microbiome project. Nat. Genet. 54:143–151. doi:10.1038/s41588-021-00992-y

Maltecca, C., D. Lu, C. Schillebeeckx, N. P. McNulty, C. Schwab, C. Shull, and F. Tiezzi. 2019. Predicting growth and carcass traits in swine using microbiome data and machine learning algorithms. Sci. Rep. 9:1–15. doi:10.1038/s41598-019-43031-x

Marcobal, A., P. C. Kashyap, T. A. Nelson, P. A. Aronov, M. S. Donia, A. Spormann, M. A. Fischbach, and J. L. Sonnenburg. 2013. A metabolomic view of how the human gut microbiota impacts the host metabolome using humanized and gnotobiotic mice. ISME J. 7:1933–1943. doi:10.1038/ismej.2013.89

Martínez-Álvaro, M., P. Hernández, and A. Blasco. 2016. Divergent selection on intramuscular fat in rabbits: Responses to selection and genetic parameters. J. Anim. Sci. 94:4993–5003. doi:10.2527/jas.2016-0590

Martínez-Álvaro, M., P. Hernández, S. Agha, and A. Blasco. 2018a. Correlated responses to selection for intramuscular fat in several muscles in rabbits. Meat Sci. 139:187–191. doi:10.1016/j.meatsci.2018.01.026

Martínez-Álvaro, M., Y. Paucar, K. Satué, A. Blasco, and P. Hernández. 2018b. Liver metabolism traits in two rabbit lines divergently selected for intramuscular fat. Animal. 12:1217–1223. doi:10.1017/S1751731117002695

Martínez-Álvaro, M., A. Zubiri-Gaitán, P. Hernández, M. Greenacre, A. Ferrer, and A. Blasco. 2021. Comprehensive functional core microbiome comparison in genetically obese and lean hosts under the same environment. Commun. Biol. 4:1246. doi:10.1038/s42003-021-02784-w

Martínez-Álvaro, M., N. Ibáñez-Escriche, and C. Casto-Rebollo. 2023. Innovation in statistical learning: friendly Bayesian inference in the R programming language. In: VII Congreso Internacional sobre Aprendizaje, Innovación y Cooperación. Zaragoza 1:32–35. doi:10.26754/CINAIC.2023.0003

Martínez-Álvaro, M., A. Zubiri-Gaitán, P. Hernández, C. Casto-Rebollo, N. Ibáñez-Escriche, M. A. Santacreu, A. Artacho, V. Pérez-Brocal, and A. Blasco. 2024. Correlated responses to selection for intramuscular fat on the gut microbiome in rabbits. Animals. 14:2078. doi:10.3390/ani14142078

Mitrić, A., and I. Castellano. 2023. Targeting gamma-glutamyl transpeptidase: A pleiotropic enzyme involved in glutathione metabolism and in the control of redox homeostasis. Free Radic. Biol. Med. 208:672–683. doi:10.1016/j.freeradbiomed.2023.09.020

Murga-Garrido, S. M., Q. Hong, T. W. L. Cross, E. R. Hutchison, J. Han, S. P. Thomas, E. I. Vivas, J. Denu, D. G. Ceschin, Z. Z. Tang, et al. 2021. Gut microbiome variation modulates the effects of dietary fiber on host metabolism. Microbiome. 9:1–26. doi:10.1186/s40168-021-01061-6

Nelson, D. L., and M. M. Cox. 2021a. Lipid biosynthesis. In: Nelson, D. L., and M. M. Cox, editors. Lehninger principles of biochemistry. 8th ed. New York (NY): W.H. Freeman and Company; p. 744–793.

Nelson, D. L., and M. M. Cox. 2021b. Biosynthesis of amino acids, nucleotides, and related molecules. In: Nelson, D. L., and M. M. Cox, editors. Lehninger principles of biochemistry. 8th ed. New York (NY): W.H. Freeman and Company; p. 794–840.

Newgard, C. B. 2012. Interplay between lipids and branched-chain amino acids in development of insulin resistance. Cell Metab. 15:606–614. doi:10.1016/j.cmet.2012.01.024

Newgard, C. B., J. An, J. R. Bain, M. J. Muehlbauer, R. D. Stevens, L. F. Lien, A. M. Haqq, S. H. Shah, M. Arlotto, C. A. Slentz, et al. 2009. A branched-chain amino acid-related metabolic signature that differentiates obese and lean humans and contributes to insulin resistance. Cell Metab. 9:311–326. doi:10.1016/j.cmet.2009.02.002

Nowak, A., M. Arabski, and Z. Libudzisz. 2008. Ability of intestinal lactic acid bacteria to bind and/or metabolise indole. Food Technol. Biotechnol. 46:299–304. https://hrcak.srce.hr/26380

Pla, M., M. Pascual, and B. Ariño. 2010. Protein, fat and moisture content of retail cuts of rabbit meat evaluated with the NIRS methodology. World Rabbit Sci. 12:149–158. doi:10.4995/wrs.2004.574

Rantala, A. O., M. Lilja, H. Kauma, M. J. Savolainen, A. Reunanen, and Y. A. Kesäniemi. 2000. Gamma-glutamyl transpeptidase and the metabolic syndrome. J. Intern. Med. 248:230–238. doi:10.1046/j.1365-2796.2000.00723.x

Ridaura, V. K., J. J. Faith, F. E. Rey, J. Cheng, A. E. Duncan, A. L. Kau, N. W. Griffin, V. Lombard, B. Henrissat, J. R. Bain, et al. 2013. Gut microbiota from twins discordant for obesity modulate metabolism in mice. Science. 341:1241214. doi:10.1126/science.1241214

Rivera-Pinto, J., J. J. Egozcue, V. Pawlowsky-Glahn, R. Paredes, M. Noguera-Julian, and M. L. Calle. 2018. Balances: a new perspective for microbiome analysis. mSystems. 3:1–12. doi:10.1128/msystems.00053-18

Roager, H. M., and T. R. Licht. 2018. Microbial tryptophan catabolites in health and disease. Nat. Commun. 9:1–10. doi:10.1038/s41467-018-05470-4

Rothschild, D., O. Weissbrod, E. Barkan, A. Kurilshikov, T. Korem, D. Zeevi, P. I. Costea, A. Godneva, I. N. Kalka, N. Bar, et al. 2018. Environment dominates over host genetics in shaping human gut microbiota. Nature. 555:210–215. doi:10.1038/nature25973

Rudolph, F. B. 1994. The biochemistry and physiology of nucleotides. J. Nutr. 124:124S–127S. doi:10.1093/jn/124.suppl_1.124S

Sheng, S., S. Yan, J. Chen, Y. Zhang, Y. Wang, Q. Qin, W. Li, T. Li, M. Huang, S. Ding, et al. 2022. Gut microbiome is associated with metabolic syndrome accompanied by elevated gamma-glutamyl transpeptidase in men. Front. Cell. Infect. Microbiol. 12:1–14. doi:10.3389/fcimb.2022.946757

Siddik, M. A. B., and A. C. Shin. 2019. Recent progress on branched-chain amino acids in obesity, diabetes, and beyond. Endocrinol Metab. 34:234–246. doi:10.3803/EnM.2019.34.3.234

Sosa-Madrid, B. S., P. Hernández, A. Blasco, C. S. Haley, L. Fontanesi, M. A. Santacreu, R. N. Pena, P. Navarro, and N. Ibáñez-Escriche. 2020. Genomic regions influencing intramuscular fat in divergently selected rabbit lines. Anim. Genet. 51:58–69. doi:10.1111/age.12873

Stekhoven, D. J., and P. Bühlmann. 2011. MissForest—nonparametric missing value imputation for mixed-type data. Bioinformatics. 28:112–118. doi:10.1093/bioinformatics/btr597

Tai, E. S., M. L. S. Tan, R. D. Stevens, Y. L. Low, M. J. Muehlbauer, D. L. M. Goh, O. R. Ilkayeva, B. R. Wenner, J. R. Bain, J. J. M. Lee, et al. 2010. Insulin resistance is associated with a metabolic profile of altered protein metabolism in Chinese and Asian-Indian men. Diabetologia. 53:757–767. doi:10.1007/s00125-009-1637-8

Taniguchi, M., A. Arakawa, M. Nishio, T. Okamura, C. Ohnishi, K. Kadowaki, K. Kohira, F. Homma, K. Matsumoto, and K. Ishii. 2020. Differential metabolomics profiles identified by CE-TOFMS between high and low intramuscular fat amount in fattening pigs. Metabolites. 10:322–315. doi:10.3390/metabo10080322

Turnbaugh, P. J., R. E. Ley, M. A. Mahowald, V. Magrini, E. R. Mardis, and J. I. Gordon. 2006. An obesity-associated gut microbiome with increased capacity for energy harvest. Nature. 444:1027–1031. doi:10.1038/nature05414

Valizadeh, A., M. Kazemi-Bonchenari, M. Khodaei-Motlagh, M. H. Moradi, and A. Z. M. Salem. 2021. Effects of different rumen undegradable to rumen degradable protein ratios on performance, ruminal fermentation, urinary purine derivatives, and carcass characteristics of growing lambs fed a high wheat straw-based diet. Small Ruminant Res. 197:106330. doi:10.1016/j.smallrumres.2021.106330

Vanweert, F., P. Schrauwen, and E. Phielix. 2022. Role of branched-chain amino acid metabolism in the pathogenesis of obesity and type 2 diabetes-related metabolic disturbances BCAA metabolism in type 2 diabetes. Nutr. Diabetes. 12:1–13. doi:10.1038/s41387-022-00213-3

Wahlström, A., S. I. Sayin, H. U. Marschall, and F. Bäckhed. 2016. Intestinal crosstalk between bile acids and microbiota and its impact on host metabolism. Cell Metab. 24:41–50. doi:10.1016/j.cmet.2016.05.005

Warner, R. D., P. L. Greenwood, D. W. Pethick, and D. M. Ferguson. 2010. Genetic and environmental effects on meat quality. Meat Sci. 86:171–183. doi:10.1016/j.meatsci.2010.04.042

Warris, P. D. 2010. Meat Quality. In: Meat science: an introductory text. 2nd Ed. Wallingford, UK: CABI; p. 77–96.

Westerhuis, J. A., H. C. J. Hoefsloot, S. Smit, D. J. Vis, A. K. Smilde, E. J. J. Velzen, J. P. M. Duijnhoven, and F. A. Dorsten. 2008. Assessment of PLSDA cross validation. Metabolomics. 4:81–89. doi:10.1007/s11306-007-0099-6

White, P. J., A. L. Lapworth, J. An, L. Wang, R. W. McGarrah, R. D. Stevens, O. Ilkayeva, T. George, M. J. Muehlbauer, J. R. Bain, et al. 2016. Branched-chain amino acid restriction in Zucker-fatty rats improves muscle insulin sensitivity by enhancing efficiency of fatty acid oxidation and acyl-glycine export. Mol. Metab. 5:538–551. doi:10.1016/j.molmet.2016.04.006

Wlodarska, M., C. Luo, R. Kolde, E. D'Hennezel, J. W. Annand, C. E. Heim, P. Krastel, E. K. Schmitt, A. S. Omar, E. A. Creasey, et al. 2017. Indoleacrylic acid produced by commensal Peptostreptococcus species suppresses inflammation. Cell Host Microbe 22:25–37. e6.e6. doi:10.1016/j.chom.2017.06.007

Xie, C., J. Teng, X. Wang, B. Xu, Y. Niu, L. Ma, and X. Yan. 2022. Multi-omics analysis reveals gut microbiota-induced intramuscular fat deposition via regulating expression of lipogenesis-associated genes. Anim. Nutr. 9:84–99. doi:10.1016/j.aninu.2021.10.010

Zarei, I., V. M. Koistinen, M. Kokla, A. Klåvus, A. F. Babu, M. Lehtonen, S. Auriola, and K. Hanhineva. 2022. Tissue-wide metabolomics reveals wide impact of gut microbiota on mice metabolite composition. Sci. Rep. 12:1–20. doi:10.1038/s41598-022-19327-w

Zhang, S., X. Zeng, M. Ren, X. Mao, and S. Qiao. 2017. Novel metabolic and physiological functions of branched chain amino acids: a review. J. Anim. Sci. Biotechnol. 8:4–15. doi:10.1186/s40104-016-0139-z

Zierer, J., M. A. Jackson, G. Kastenmüller, M. Mangino, T. Long, A. Telenti, R. P. Mohney, K. S. Small, J. T. Bell, C. J. Steves, et al. 2018.

The fecal metabolome as a functional readout of the gut microbiome. Nat. Genet. 50:790–795. doi:10.1038/s41588-018-0135-7

Zomeño, C., A. Blasco, and P. Hernández. 2013. Divergent selection for intramuscular fat content in rabbits. II. Correlated responses on carcass and meat quality traits. J. Anim. Sci. 91:4532–4539. doi:10.2527/jas.2013-6417

Zubiri-Gaitán, A., A. Blasco, R. Ccalta, K. Satué, and P. Hernández. 2022a. Intramuscular fat selection in rabbits modifies the fatty acid composition of muscle and liver tissues. Animals. 12:893–812. doi:10.3390/ani12070893

Zubiri-Gaitán, A., M. Mora, C. Casto-Rebollo, M. A. Santacreu, A. Blasco, P. Hernandez, and N. Ibañez-Escriche. 2022b. Maternal effect on the metagenomic composition determining the intramuscular fat content in rabbits. In: R. F. Veerkamp and Y. de Haas, editors. 12th World Congress on Genetics Applied to Livestock Production. Rotterdam: Wageningen Academic Publishers; p. 2073–2076.

Zubiri-Gaitán, A., A. Blasco, and P. Hernández. 2023. Plasma metabolomic profiling in two rabbit lines divergently selected for intramuscular fat content. Commun. Biol. 6:893. doi:10.1038/s42003-023-05266-3